Investigation of Photocatalytic Activity of Nd-Doped ZnO Nanoparticles Using Brilliant Green Dye: Synthesis and Characterization

Gnanaprakasam, Arul Jesu; Sivakumar, Vaiyazhipalayam Murugaiyan *+; Thirumarimurugan, Marimuthu

Department of Chemical Engineering, Coimbatore Institute of Technology, Coimbatore – 641 014, Tamil Nadu, INDIA

ABSTRACT: *An Nd doped ZnO (1-5%) photocatalyst was successfully synthesized via chemical co-precipitation method. The optical property, nature, and morphology of the synthesized nanoparticles were analyzed by UV-Visible, XRD, and FESEM respectively. XRD study reveals that Nd has been effectively incorporated in the ZnO lattice in the lower level dosage; however the crystalline nature has been distorted towards the increase in the Nd. The selected brilliant green dye was degraded photo-catalytically with the help of the synthesized nanoparticles and the study has been extended with catalyst dosage and dye concentration. The 2% Nd-doped ZnO showed a remarkable result of 98.26% degradation of brilliant green dye compared to the other 1,3,4 & 5 % Nd-doped ZnO nanoparticles which clearly indicates the optimization of depletion region corresponding to the maximum degradation. The increased content (3-5%) of Nd-doped ZnO exhibited moderate photocatalytic degradation of the dye due to the decreased crystalline nature which was further evidenced from XRD studies.*

KEYWORDS: *Nd-doped ZnO nanoparticles; Brilliant green dye; Kinetic study; Photocatalytic degradation.*

INTRODUCTION

Effluents discarded from the textiles, paper, pulp and paint industries contain toxic constituents like dyes, pigments etc. These constituents are more toxic and recalcitrant in nature. Among various dyes, azo dyes are the most used synthetic dye stuff and it is characterized by aromatic compounds linked with one or more azo functional groups (R_1-N = N-R_2). These dyes remain chemically stable in the waste water after treatments due to the presence of azo and sulfo functional groups [1]. Among the various azo dyes, Brilliant Green dye is one among the most used dyes in various industries. In spite of its worldwide applications, it roots to cancer, respiratory & mutagenesis diseases. In addition to that, it projects hazardous effects in the reproductive and immune systems of the living systems [2,3]. There are various treatment technologies available to treat these azo dyes containing effluents through physical, chemical and biological methods. Among them, advanced oxidation

***** *To whom correspondence should be addressed.*
+ E-mail: vmsivakumar@gmail.com
1021-9986/2018/2/61-71 11/$/6.01

process (AOP) emerges as one of a most promising method for the treatment of organic dye effluent [4]. Because this technique has many advantages over conventional treatment methods such as it convert all the toxic dye effluent into harmless products [5].

The photocatalytic degradation of organic effluent was recognized as an effective tool to eradicate the environmental problems which were originated from the presence of azo dyes in the effluent water [6]. Recently, semiconductors such as TiO_2, ZnO, SnO_2, and WO_3 have been utilized as a photocatalyst for the degradation of organic effluents [7-10]. TiO_2 have been used by most of the researchers, because of its chemical stability and easy availability. However, ZnO is emerged as most attractive photocatalyst due to its advantage over TiO_2 catalyst such as low cost, chemical stability, wide band gap (3.2ev), high exciton binding energy (60 meV) and eco-friendly nature [11].

Doping is an efficient and simplest technique to enhance the photocatalytic behavior of prepared nano-photocatalyst. Doping changes the surface area of prepared nanocatalyst and the amalgamation of dopant ions in the ZnO lattice induces lattice defects which results in better photocatalyst than pure metal oxide catalyst [12]. Introducing dopant in the photocatalyst reduces the band gap energy of prepared photocatalyst which further improves the photocatalytic behavior under UV-Visible region. Moreover, lattice defects introduce split into the energy levels that yield the better photocatalyst in the removal of toxic contaminants in the wastewater [13, 14]. Doping of ZnO with metal and nonmetals are the best way to generate defects, so that optical property of the prepared catalyst can be enhanced [15, 16]. Recently, rare earth metals have emerged as excellent dopants to improve the photocatalytic activity of ZnO [17-21]. Among the lanthanide series, Nd received tremendous attention due to its improved optical properties and better photocatalytic activity.

To the best of our knowledge, a very few researchers have reported the photocatalytic degradation of organic dye effluents using Nd doped ZnO via co-precipitation method, such as photocatalytic activity of Nd-doped ZnO NPs towards methyl orange dye synthesized through hydrothermal method [11], Nd-doped ZnO thin film towards the degradation of methylene blue dye synthesized via sol-gel spin coating method [20], Nd-doped ZnO hierarchical micro/nanospheres in the degradation of phenol *via* simple chemical precipitation method [19] and Nd-doped ZnO NPs in the degradation of 4-nitrophenol synthesized via the polyacrylamide-gel method [25].

In this present research work, pure and (1-5 %) Nd-doped ZnO NPs capped with PVP were synthesized successfully *via* chemical co-precipitation method and the photocatalytic activity of the prepared photocatalyst was examined with brilliant green dye under UV-Visible irradiation. The synthesized nanoparticles were characterized by UV-Vis spectrophotometer, XRD, FE-SEM with EDX. Furthermore, the effect of initial dye concentration and catalyst dosage was extensively studied and reported.

EXPERIMENTAL SECTION

Materials

Zinc sulphate heptahydrate ($ZnSO_4.7H_2O$) and PVP (agglomeration preventing agent) were purchased from SD Fine Chem Ltd. India, Neodymium acetate monohydrate was purchased from Sigma-Aldrich, USA. Sodium hydroxide (NaOH) was procured from Merck, India All the other chemicals used were analytical grade and used without any further purification. Double distilled water was used throughout the experiments.

Synthesis of Nd-doped ZnO nanoparticles

About 7.19 g (0.25 M) of $ZnSO_4$ was dissolved in 100 mL distilled water followed by the addition of 0.041 g (1%) of Neodymium (III) acetate monohydrate and stirred for 30 min. After the stipulated time, 100 mL of 1 wt % PVP solution was added to the above mixture and the stirring was again continued for 30 min. Then, 60 mL of 0.5 M of NaOH was added dropwise to the above mixture and a white precipitate was obtained. Then, the stirring was continued for the next 30 min for the completion of the reaction. Further, the obtained precipitate was centrifuged, washed twice with ethanol and distilled water and dried at 100 ^{O}C for 6 h followed by the calcination at 350 °C for 3 h. The same procedure was adopted for the synthesis of pure and (2-5%) of Nd-doped ZnO NPs.

Characterizations

The synthesized nanoparticles were characterized by X-ray diffraction using Shimadzu XRD 6000 with

Cu -Kα radiation at 40 kV (Japan) to study the crystalline nature of the synthesized nanoparticles. Field Emission Scanning Electron Microscopy (FESEM) and Energy Dispersive Spectra (EDS) analysis were performed to determine the surface morphology and elemental compositions of the NPs using SIGMA HV – Carl Zeiss with Bruker Quantax 200 – Z10 EDS Detector. The absorbance was performed with a UV-Visible spectrophotometer (Merck, USA) to determine the band gap and photocatalytic activity of the synthesized nanoparticles.

Photocatalytic activity on Brilliant green dye

About 10 ppm of 100 mL of BG dye solution was taken into 250 mL beaker along with 0.25 g of synthesized nano-photocatalyst. The reaction mixture was stirred under the dark condition for the 30 min to establish the adsorption-desorption equilibrium. After the stipulated period, the UV-Visible light source was provided to the mixture and the stirring was continued. At every 30 minutes, the samples were centrifuged and analyzed with a UV-Visible spectrophotometer (λ_{max} = 630 nm) to measure the absorption. The percentage removal of dye was determined using the following equation,

$$\% \text{ Removal of dye} = \frac{A_0 - A}{A_0} \times 100 \quad (1)$$

Where,

A_0 is the initial absorption of supernatant (after 30 min stirring at dark condition).

A is the absorption of the supernatant at a stipulated time period.

RESULTS AND DISCUSSION

Optical study

UV-Vis absorption spectra of the synthesized undoped and (1-5 %) Nd-doped ZnO NPs capped with PVP is shown in Fig. 1(a). The UV-Vis absorption spectrum exhibits a strong excitonic peaks at 375, 375, 373, 372, 374 and 373 nm for undoped and 1 - 5 % Nd-doped ZnO NPs respectively, and these strong excitonic peaks result from the movement of electrons from valence band to conduction band which reveals the good optical property and high exciton binding energy of synthesized photocatalyst [22]. The synthesized (2-5 %) Nd-doped ZnO exhibits a blue shift with respect to pure ZnO NPs, except for 1 % Nd-doped ZnO NPs. Moreover, it was observed that all the synthesized ZnO NPs has shown good absorption light in the visible region. Among the synthesized ZnO NPs, 2 % Nd doped ZnO exhibits better absorption of visible light. The band gap of prepared ZnO NPs were calculated using Tauc's equation which establishes the relation between incident light energy (hν) and co-efficient of absorption (α) as given below,

$$\alpha = \frac{A(h\upsilon - E_g)^n}{h\upsilon} \quad (2)$$

Where, n is constant which depends on nature of transition, n=1/2,3/2,2,3 for direct allowed, direct for forbidden, indirect allowed, indirect forbidden transitions respectively and *A* is constant. Since ZnO is direct allowed transition material, n is taken as ½. The band gap energy has been calculated using tauc's plot in which the liner portion of the $(\alpha h\nu)^2$ *vs* hν graph (Fig. 1(b)). The calculated bag gap values are 3.09 eV, 3.00 eV, 2.82 eV, 2.776 eV, 2.84 eV and 2.85 eV for undoped and 1 - 5% Nd doped ZnO respectively. It has been noticed that the band gap of Nd-doped ZnO NPs decreases for 1-3% Nd doping however, the values tend to increase gradually for 4-5% Nd-doped ZnO. This may be due to two reasons (i) Nd^{3+} ions can act as donor or acceptor, (ii) the small quantity of Nd^{3+} ions may create the energy level near to the conduction band or valence band and thus causes the reduction in the band gap energy value in the Nd-doped ZnO NPs. Since, ZnO is an n-type semiconductor, due to Burstein-moss effect, the excesses of charge carrier and shifts in the Fermi level inside the conduction band may increase the band gap energy, if the dopant concentration was increased beyond the optimum doping level.

XRD studies

The XRD pattern of PVP capped pure and (1–5 %) Nd-doped ZnO NPs are shown in Fig. 2. The diffraction peaks confirm the synthesized nanoparticles possess hexagonal wurtzite structure (ICDD No. 36-1451). The broadening of XRD diffraction peaks of (1-5 %) Nd-doped ZnO NPs with respect to pure ZnO NPs was observed which might be due to the increase in a doping concentration of Nd^{3+} and also by replacing the interstitial Zn. Further, the incorporation of Nd^{3+} inhibits the crystalline structure of ZnO which would result lattice

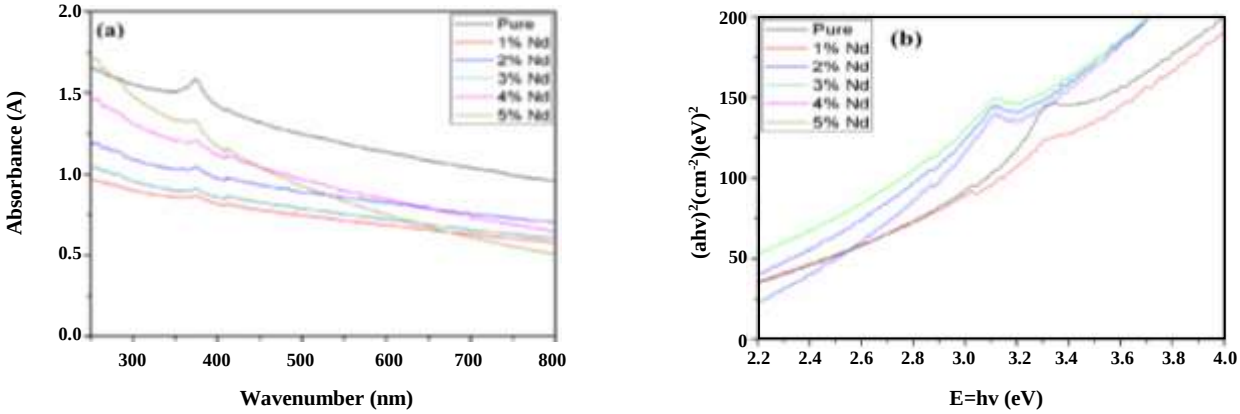

Fig. 1: (a). UV–Visible absorption spectra of Pure and (1-5 %) Nd-doped ZnO NPs, (b). Tauc's plot for pure and (1-5 %) Nd doped ZnO NPs.

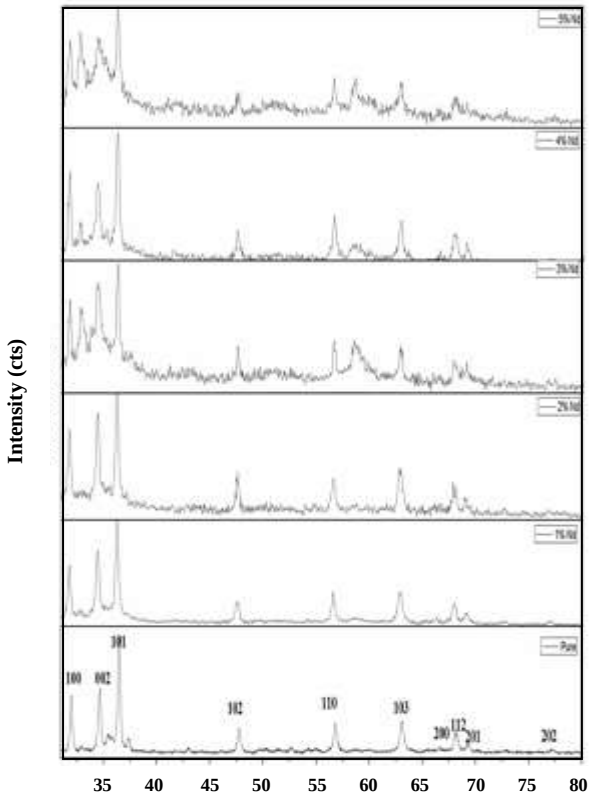

Fig. 2: XRD pattern Pure and (1-5 %) Nd-doped ZnO NPs.

disorder and related stress [15]. The average crystallite size of the synthesized pure and doped ZnO NPs was calculated using the Debye Scherer equation.

$$D_p = \frac{0.9\lambda}{\beta \cos\theta} \quad (3)$$

Where D_p is the average particle size (nm), β is the full width at half maximum (FWHM) (radian), θ is Bragg angle (radian) and λ is wavelength (nm). The average particle size is 68.01 nm for pure, 33.26 nm for 1 % Nd, 38.136 nm for 2 % Nd, 36.27 nm for 3 % Nd, 36.28 nm for 4 % Nd and 39.20 nm for 5 % Nd-doped ZnO NPs respectively. The size of (1-5 %) Nd-doped ZnO NPs was found to decrease compared to pure ZnO NPs. This might result from the formation of Nd-O-Zn on the surface of ZnO NPs which inhibits agglomeration of nanoparticles [23-25].

A significant shift in the diffraction peak positions was observed towards lower value for (1-5 %) Nd-doped ZnO NPs compared to pure ZnO particles. Since, the ionic radius of Nd^{3+} (0.143 nm) is greater than Zn^{2+} (0.074 nm) ions, the diffraction peak shifts towards the lower angle [18, 26]. It reveals that incorporation of Nd in the ZnO lattice affects the crystalline structure of the prepared nanoparticles. However, no such significant shifts in the peak positions were observed between 1-5 % Nd-doped ZnO NPs.

FE-SEM and EDS studies

FE-SEM images of the pure and 2 % doped ZnO NPs are shown in Fig. 3 (a) and (b) respectively. It is observed that pure ZnO NPs exhibits micro flower nanoleaf like morphology, but 2 % Nd-doped ZnO NPs morphology exhibits disorganized leaf-like structure which deviates from the pure ZnO NPs which is in accordance with XRD analysis. Energy dispersive spectrum of prepared (1-5 %) Nd-doped ZnO is shown in Fig. 4 (a-f) which confirms

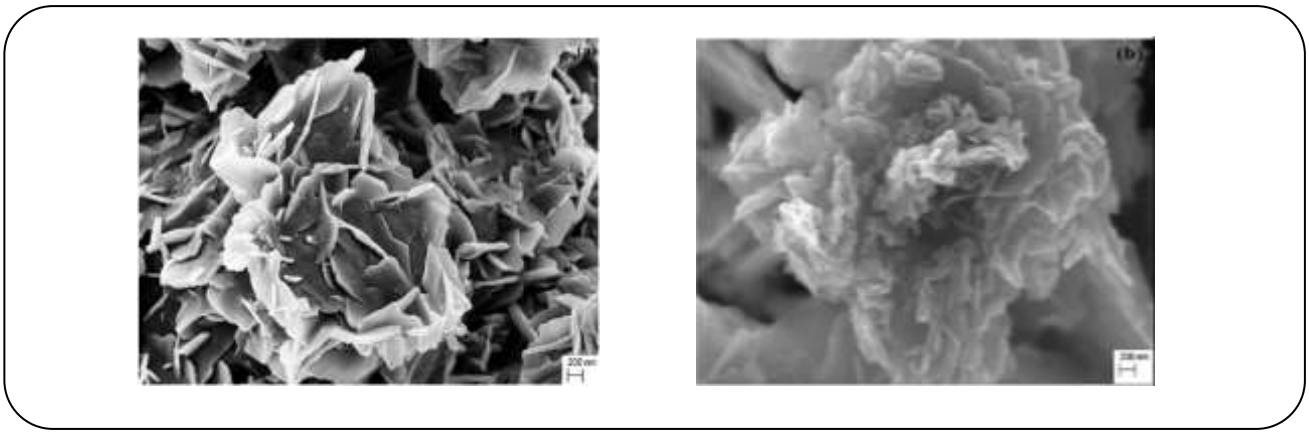

Fig. 3: FESEM images (a). Pure ZnO NPs (b). 2 % Nd-doped ZnO NPs.

the presence of Nd dopant in the prepared ZnO nanoparticles and the presence of sulphur and carbon which were resulted from the incomplete conversion of $ZnSO_4$ into $Zn(OH)_2$ and PVP capping agent respectively.

Photocatalytic studies

The photocatalytic activity of pure and (1-5 %) Nd-doped ZnO was tested with brilliant green dye under UV-Visible light and the results are shown in Fig. 5. It was noticed that 88.6% removal of dye for pure ZnO NPs under UV-Visible light was observed in 3 h. Increase in the removal percentage of BG dye was resulted by an increase in the dopant concentration till 2 % Nd. Then the removal percentage was begun to decrease gradually from 3 to 5 % Nd dopant concentration due to the effect of dopant concentration (the recombination of a hole and excited electron) on the photocatalytic activity of the synthesized nanocatalyst is discussed as follow,

Illumination of light on the on the pure ZnO, suspended in the dye solution with energy more than or equal to the band gap energy which excites the electrons ($e^-_{(cb)}$) from the valence band to conduction band by leaving holes ($h^+_{(vb)}$) in the valence band.

$$ZnO + h\nu \rightarrow e^-_{(cb)} + h^+_{(vb)}$$

Further, the photoinduced $e^-_{(cb)}$ combines with dissolved O_2 and promotes the following reaction scheme,

$$O_2 + e^-_{(cb)} \rightarrow O_2^{\bullet-}$$

$$O_2^{\bullet-} + H_2O \rightarrow HO_2\bullet + OH^-$$

Similarly, the photoinduced holes ($h^+_{(vb)}$) combines with either hydroxyl ions (OH^-) or water molecules (H_2O) to result in the following reactions,

$$h_{vb}^+ + OH^- \rightarrow OH\bullet$$

$$h_{vb}^+ + H_2O \rightarrow OH\bullet + H^+$$

Both the hydroperoxy radical ($HO_2\bullet$) and hydroxyl radical ($OH\bullet$) are a strong oxidizing agent which roots the degradation of organic dye molecules. However, the recombination of a hole and excited electron might result in the reduction of photocatalytic activity [27].

$$e_{cb}- + h_{vb}^+ \rightarrow ZnO$$

The substitution of Nd^{3+} ions in the ZnO lattice with partially filled f-orbital promotes multi-energy levels between the conduction band and valence band. Further, Nd^{3+} ions attract photoinduced $e^-_{(cb)}$ to form Nd^{2+} which prevents the $e_{cb}-$ and h_{vb}^+ recombination which increases photocatalytic activity of synthesized Nd doped ZnO. In addition, Nd^{2+} ions might react with O_2 to endorse the generation of the superoxide, which further improves the photocatalytic activity of the prepared Nd doped ZnO NPs.

$$Nd^{3+} + e^- \rightarrow Nd^{2+}$$

$$Nd^{2+} + O_2 \rightarrow Nd^{3+} + O_2^{-\bullet}$$

Moreover, the increase in the doping percentage enhances surface barrier and narrows the space charge leads to the separation of photoinduced electron-hole. Also, doping of Nd^{3+} ions in ZnO lattice enhances the absorbance of OH^- on the surface of the ZnO nanocatalyst due to the presence of oxygen vacancies. The surface adsorbed OH^- act as a strong tool to trap the photo

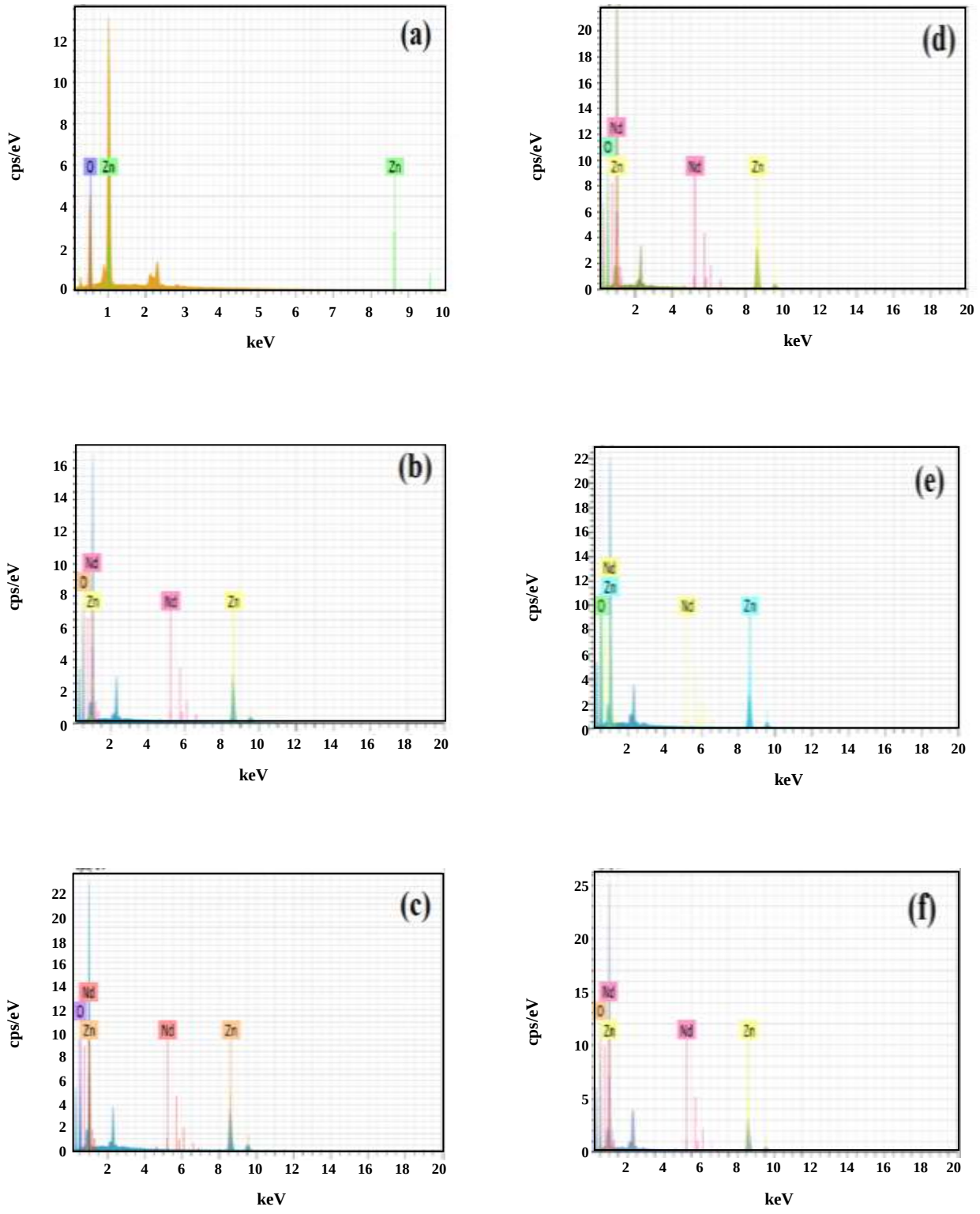

Fig. 4: Energy dispersive spectra (a). Pure (b). 1 % Nd-doped (c). 2 % Nd-doped (d). 3 % Nd-doped (e). 4 % Nd-doped (f). 5 % Nd doped ZnO NPs.

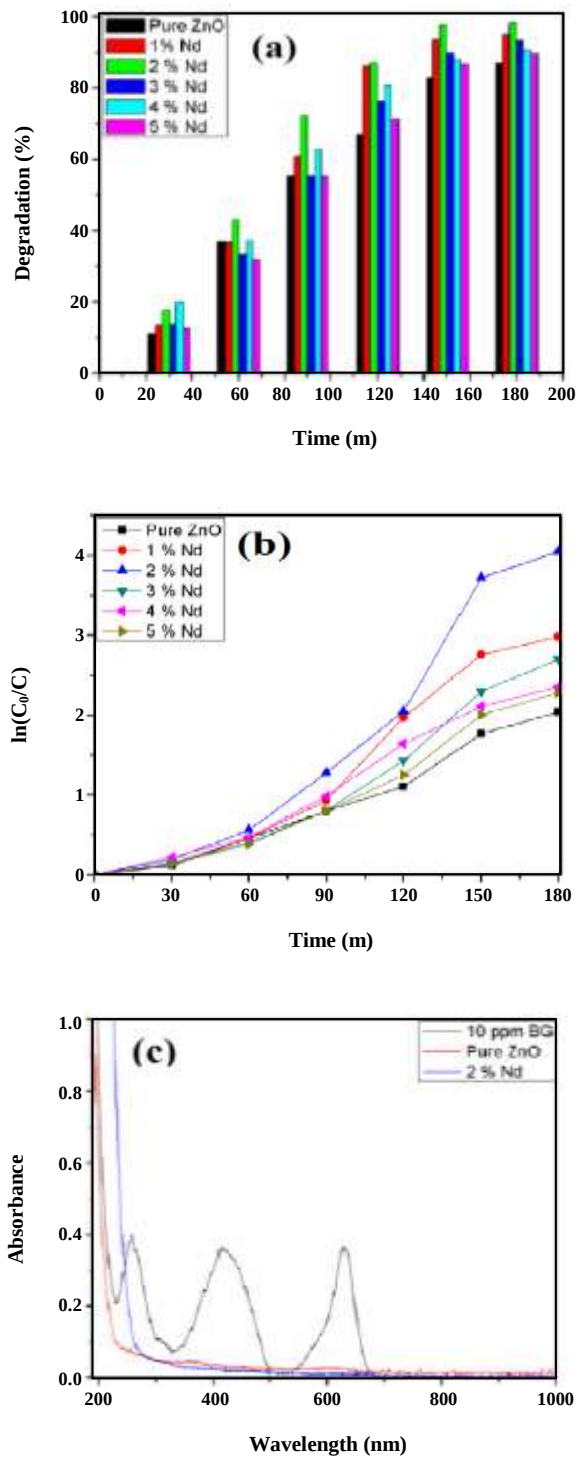

Fig. 5: (a). Percentage removal of BG dye with respect to time for Pure and (1-5 %) doped ZnO NPs (b.) kinetics of brilliant green dye degradation for Pure and (1-5 %) doped ZnO NPs ZnO NPs and (c). The absorption spectrum of Brilliant Green dye aqueous solution for 3 h duration degraded by pure and (1-5 %) doped ZnO NPs.

induced holes [28]. However, beyond the optimum doping level (2 % Nd), light penetration depth into ZnO NPs exceeds the space charge region which increases the possibility of recombination of photoinduced electron-holes pairs. Therefore, a decrease in the photocatalytic degradation was obtained [29]. In this case, the above phenomena demand the optimum doping level for the penetration depth of light and charge separation region which should be equal. Furthermore, the optimum level of doping is needed to create a potential difference between the recombination center and surface of the particles to reduce the recombination of photogenerated electron-hole pairs.

The kinetics of the photocatalytic degradation of BG dye using pure and (1-5 %) doped ZnO nanoparticles follows the pseudo-first order.

$$-\ln(C/C_0) = \ln(C_0/C) = kt \quad (4)$$

Where C_0 and C are the initial concentration and concentration at time t respectively and k is the reaction rate constant. Fig 4(b) furnish the relationship between $\ln(C_0/C)$ *vs* time and the rate constant k (min^{-1}) and linear regression coefficient R (Table 1).

Effect of photocatalyst dosage

The effect of catalyst loading on the photocatalytic activity of prepared photocatalyst is studied by varying catalyst concentration ranging from 2.0 to 4.0 g/L and the results are observed in Fig. 6. It was found that the k value increases till 2.5 g/L because the higher concentration leads to increased availability of adsorption surface and enhanced induction of oxidizing radicals (Table 2). However, the k value is decreased gradually from 3.0 to 4 g/L due to the increased concentration of catalyst which leads to the enhancement of turbidity of the aqueous solution; hence, a reduction of availability of photons occurs for the degradation of organic molecules [30].

Effect of initial dye concentration

The influence of initial dye concentration on the photocatalytic behavior of synthesized 2 % Nd-doped ZnO was examined by ranging the initial dye concentration from 10 mg/L to 50 mg/L and results are presented in Table 3. It was noticed that k values decrease with the increase in initial dye concentration (Fig. 7). Because the higher concentration of dye molecules yields enhanced adsorption on the catalyst surface which diminishes the generation of

Table 1: Reaction rate constant of BG degradation and regression coefficient for Pure, and (1-5 %) doped ZnO NPs.

S.No	Catalyst	k (Reaction rate constant/min)	R^2(Regression coefficient)
1	Pure ZnO	0.012	0.972
2	1 % Nd doped ZnO	0.015	0.918
3	2 % Nd doped ZnO	0.020	0.899
4	3 % Nd doped ZnO	0.013	0.914
5	4 % Nd doped ZnO	0.013	0.963
6	5 % Nd doped ZnO	0.011	0.933

Table 2. Pseudo first-order rate constant of photocatalytic degradation of BG dye and regression coefficient for the different catalyst dosage of 2 % Nd-doped ZnO NPs at 10 ppm initial dye concentration.

S.No	Catalyst loading (g/L)	k (Reaction rate constant/min)	R^2 (Regression coefficient)
1	2.0	0.007	0.891
2	2.5	0.014	0.899
3	3.0	0.011	0.932
4	3.5	0.011	0.935
5	4.0	0.08	0.913

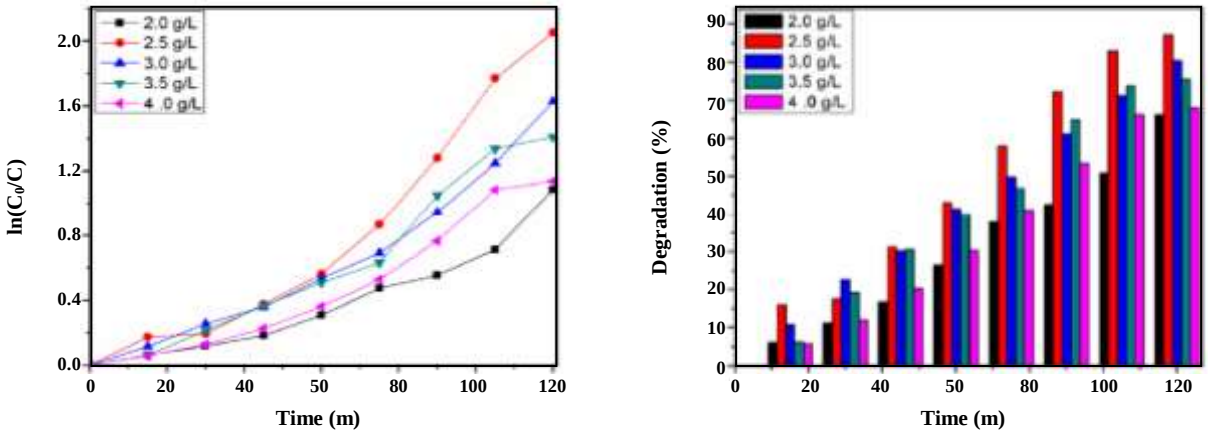

Fig. 6: Influence of catalyst loading on the photocatalytic degradation of BG dye using 2 % Nd-doped ZnO NPs. (a). ln (C_0/C) vs time (b). % Degradation.

hydroxyl radicals. In addition, at the increased BG dye concentration, the number of photons reached the surface is reduced. Thus results in the reduction of the photocatalytic degradation efficiency of the synthesized nanocatalyst [31, 32].

CONCLUSIONS

Nd-doped ZnO NPs were successfully synthesized in different compositions using PVP as a capping agent *via* chemical co-precipitation method. The substitution of Nd^{3+} ions in the ZnO lattice has a distinct effect on the optical property, crystalline structure, and morphology of prepared ZnO NPs. Among the other compositions, 2 % Nd-doped ZnO NPs had shown a profound photocatalytic activity towards the selected BG dye. The influence of catalyst dosage and initial concentration of dye was studied for 2 % Nd-doped ZnO NPs and it was found that 2.5 g/L catalyst loading and 10 ppm of initial dye concentration

Table 3: Pseudo-first order rate constant of photocatalytic degradation of BG dye and regression coefficient for 2.5 g/L of 2 % Nd-doped ZnO NPs at different initial dye concentration.

S.No	Initial dye concentration (ppm)	k (Reaction rate constant)(min^{-1})	R^2(Regression coefficient)
1	10	0.014	0.899
2	20	0.004	0.984
3	30	0.002	0.989
4	40	0.002	0.982
5	50	0.001	0.985

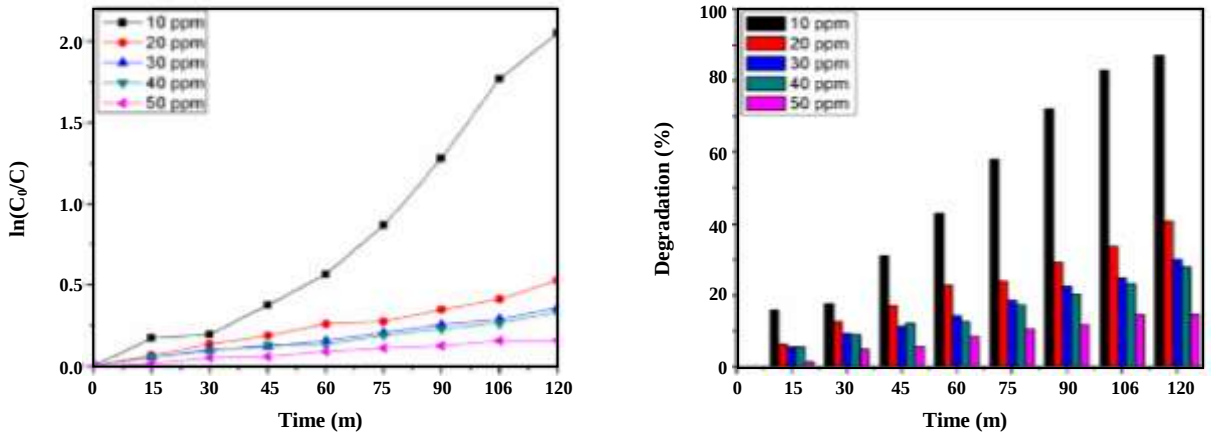

Fig. 7: Effect of initial concentration of BG dye on the photocatalytic activity of 2 % Nd-doped ZnO NPs.

results excellent removal percentage of BG dye. Hence, the obtained results would suggest the synthesized Nd doped ZnO nanoparticles could act as an excellent dye degrading agent in textile and other industries to keep the environment clean and green.

Acknowledgment

The authors convey sincere thanks to the Management and Principal of Coimbatore Institute of Technology, Coimbatore – 641 014 for providing facilities and support through Technical Education Quality Improvement Programme (TEQIP- II) fund.

Received : Dec. 17, 2015; Accepted : Mar. 12, 2018

REFERENCES

[1] Kumar N., Reddy C.N., Mohan S.V., Biomineralization of Azo Dye Bearing Wastewater in Periodic Discontinuous Batch Reactor: Effect of Microaerophilic Conditions on Treatment Efficiency, *Bioresour. Tech.*, **188**: 56–64 (2015).

[2] Shah A.T., Din M.I., Kanwal F.N., Mirza M.L., Direct Synthesis of Mesoporous Molecular Sieves of Ni-SBA-16 by Internal pH Adjustment Method and Its Performance for Adsorption of Toxic Brilliant Green Dye, *Arab J. Chem.*, **8**: 579–586 (2014).

[3] Mittal A., Kaur D., Mittal J., Applicability of Waste Materials-Bottom Ash and Deoiled Soya as Adsorbents for the Removal and Recovery of a Hazardous Dye, Brilliant Green, J. *Colloid Interface Sci.*, **326**: 8–17 (2008).

[4] Saleha T.A., Gondalb M.A., Drmoshb Q.A., Yamanib Z.H., Lyamanic A.A., Enhancement in Photocatalytic Activity for Acetaldehyde Removal by Embedding ZnO Nano Particles on Multiwall Carbon Nanotubes, *Chem. Eng. J.*, **166**: 407–412 (2011).

[5] Senthilvelan S., Chandraboss V.L., Karthikeyan B., Natanapatham L., Murugavelu M., TiO_2, ZnO and Nanobimetallic Silica Catalyzed Photodegradation of Methyl Green, *Mater. Sci. Semicond. Process*, **16**: 185–192 (2013).

[6] Gogate P.R., Pandit A.B., A Review of Imperative Technologies for Wastewater Treatment II:Hybrid Methods, *Adv. Environ. Res.*, **8**: 553–597 (2004).

[7] Długosz M., ˙Zmudzki P., Kwiecien A., Szczubiałka K., Krzek J., Nowakowska M., Photocatalytic Degradation of SulfaMethoxazole in Aqueous Solution Using a Floating TiO_2-Expanded Perlite Photocatalyst, *J. Hazard. Mater.*, **298**: 146–153 (2015).

[8] Huang J., Liu S., Kuang L., Zhao Y., Jiang T., Liu S., Xu X., Enhanced Photocatalytic Activity of Quantum-Dot-Sensitized One-Dimensionally-Ordered ZnO Nanorod Photocatalyst, *J. Environ. Sci.*, **25**: 2487–2491 (2013).

[9] Fakhri A., Behrouz S., Photocatalytic Properties of Tungsten Trioxide (WO_3) Nanoparticles for Degradation of Lidocaine under Visible and Sunlight Irradiation, *Sol. Energy*, **112**: 163–168 (2015).

[10] Luo Q., Wang L., Wang D., Yin R., Li X., An J., Yang X., Preparation, Characterization and Visible-Light Photocatalytic Performances of Composite Films Prepared from Polyvinyl Chloride and SnO_2 Nanoparticles, *J. Environ. Chem. Eng.*, **3**: 622–629 (2015).

[11] Zhao Z., Song J., Zheng J., Lian J., Optical Properties and Photocatalytic Activity of Nd-Doped ZnO Powders, *Trans. Nonferrous Met. Soc. China*, **24**: 1434−1439 (2014).

[12] Ullah R., Dutta J., Photocatalytic Degradation of Organic Dyes with Manganese-Doped ZnO Nanoparticles, *J. Hazard. Mater.*, **156**: 194-200 (2008).

[13] Kamat P.V., Huehn R., Nicolaescu R., A "Sense and Shoot" Approach for Photocatalytic Degradation of Organic Contaminants in Water, *J. Phys. Chem. B*, **106**: 788-794 (2002).

[14] Lin B., Fua Z., Green Luminescent Center in Undoped Zinc Oxide Films Deposited on Silicon Substrates, *Appl. Phys. Lett.*, **79**: 943-945 (2001).

[15] BaAbbad M.M., Kadhum A.A.H., Mohamad A.B., Takriff M.S., Sopian K., Visible Light Photocatalytic Activity of Fe^{3+}-Doped ZnO Nanoparticles Prepared via Sol–Gel Technique, *Chemosphere*, **91**: 1604-1611 (2013).

[16] Peng X., Yang B., Chu J., Feng P., Effects of Nitrogen Pressure During Pulsed Laser Deposition on Morphology and Optical Properties of N-Doped ZnO Nanostructures, *Surf. Sci.*, **609**: 48-52 (2013).

[17] Rani T.D., Tamilarasan K., Elangovan E., Leela S., Ramamurthi K., Thangaraj K., Himcinschi C., Trenkmann I., SchuIze S., Hietschold M., Liebig A., Salvan G., Zahn D.R.T., Structural and Optical Studies on Nd Doped ZnO Thin Films, *Superlattices Microstruct.*, **77**: 325–332 (2015).

[18] Zong Y., Li Z., Wang X., Ma J., Menn Y., Synthesis and High Photocatalytic Activity of Eu-Doped ZnO Nanoparticles, *Ceram. Int.*, **40**: 10375–10382 (2014).

[19] Sin J., Lam S., Lee K., Mohamedn A.R., Preparation of Rare Earth-Doped ZnO Hierarchical Micro/ Nanospheres and their Enhanced Photocatalyticactivity under Visible Light Irradiation, *Ceram. Int.*, **40**: 5431–5440 (2014).

[20] Poongodia G., Kumar R.M., Jayavel R., Structural, Optical and Visible Light Photocatalytic Properties of Nanocrystalline Nd Doped ZnO Thin Films Prepared by Sol-Gel Spin Coating Method, *Ceram. Int.*, **41**: 4169–4175 (2015).

[21] Armelao L., Quici S., Barigelletti F., Accorsi G., Bottaro G., Cavazzini M., Tondello E., Design of Luminescent Lanthanide Complexes: From Molecules to Highly Efficient Photo-Emitting Materials, *Coord. Chem. Rev.*, **254**: 487–505 (2010).

[22] Chauhan S., Kumar M., Chhoker S., Katyal S.C., Awana V.P.S., Structural, Vibrational, Optical and Magnetic Properties of Sol–Gel Derived Nd Doped ZnO Nanoparticles, *J. Mater. Sci: Mater Electron.*, **24**: 5102–5110 (2013).

[23] Anandan S., Vinu A., Mori T., Gokulakrishnan N., Srinivasu P., Murugesan V., Ariga K., Photocatalytic Degradation of 2,4,6-Trichlorophenol Using Lanthanum Doped ZnO in Aqueous Suspension, *Catal. Commun.*, **8**: 1377–1382 (2007).

[24] John R., Rajakumari R., Synthesis and Characterization of Rare Earth Ion Doped Nano ZnO, *Nano-Micro Lett.*, **4**: 65-72 (2012).

[25] Khatamiana M., Khandara A.A., Divbanda B., Haghighib M., Ebrahimiasl S., Heterogeneous Photocatalytic Degradation of 4-Nitrophenol in Aqueous Suspension by Ln (La^{3+}, Nd^{3+} or Sm^{3+}) Doped ZnO Nanoparticles, *J. Mol. Catal. A: Chem.*, **365**: 120– 127 (2012).

[26] Hosseini S.M., Abdolhosseini Sarsari I., Kameli P., Salamati H., Effect of Ag Doping on Structural, Optical, and Photocatalytic Properties of ZnO Nanoparticles, *J. Alloys Compd.*, **640**: 408–415 (2015).

[27] Tan Y.N., Wong C.L., Mohamed A.R., An Overview on the Photocatalytic Activity of Nano-Doped-TiO_2 in the Degradation of Organic Pollutants, ISRN Materials Science Volume 2011, Article ID 261219, 18 Pages, http://dx.doi.org/10.5402/2011/261219

[28] Weber A.S., Grady A.M., Koodali R.T., Lanthanide Modified Semiconductor Photocatalysts, *Catal. Sci. Technol.*, **2**: 683–693 (2012).

[29] Zhou Y., Lu S.X., Xua W.G., Photocatalytic Activity of Nd-Doped ZnO for the Degradation of C.I. Reactive Blue 4 in Aqueous Suspension Environ, *Prog. Sustain*, **28**: 226-233(2009).

[30] Saien J., Ojaghloo Z., Soleymani A.R., Rasoulifard M.H., Homogeneous and Heterogeneous AOPs for Rapid Degradation of Triton X-100 in Aqueous Media *via* UV Light, Nano Titania Hydrogen Peroxide and Potassium Persulfate, *Chem. Eng. J.*, **167**: 172–182 (2011).

[31] Mai F.D., Lu C.S., Wu C.W., Huang C.H., Chen J.Y., Chen C.C., Mechanisms of Photocatalytic Degradation of Victoria Blue R Using Nano-TiO_2**.** *Sep. Purif. Techno.*, **62**: 423-436 (2008).

[32] Pouretedal H.R., Norozi A., Keshavarz M.H., Semnani A., Nanoparticles of Zinc Sulfide Doped with Manganese, Nickel and Copper as Nanophotocatalyst in the Degradation of Organic Dyes, *J. Hazard. Mater.*, **162**: 674-681 (2009).